

Engineering Bacteria-Activated Multifunctionalized Hydrogel for Promoting Diabetic Wound Healing

Yifei Lu, Haisheng Li, Jing Wang,* Mengyun Yao, Yuan Peng, Tengfei Liu, Zhou Li,* Gaoxing Luo,* and Jun Deng*

Engineering therapeutic angiogenesis in impaired tissues is critical for chronic wound healing. Materials can be engineered to deliver specific biological cues that enhance angiogenesis. However, currently available materials have limitations for use in angiogenesis engineering since the complex inflammation environment of wounds requires spatiotemporal control. Immune cells are the central component of wound microenvironment and orchestrate immune responses to wound healing. This study presents a novel approach of using a delivery system comprising living *Lactococcus*, incorporated in a heparin-ploxamer thermoresponsive hydrogel, designed to bioengineer the wound microenvironment and enhance the angiogenesis in a highly dynamic-temporal manner. The living system can produce and protect vascular endothelial growth factor (VEGF) to increase proliferation, migration, and tube formation of endothelial cells, as well as secrete lactic acid to shift macrophages toward an anti-inflammatory phenotype, resulting in successful angiogenesis in diabetic wounds. Further, the delivery system confines the bacterial population to wounds, thereby minimizing the risk of systemic toxicities. Therefore, this living hydrogel system can be harnessed for safe and efficient delivery of therapeutics that drive the wound microenvironment toward rapid healing and may serve as a promising scaffold in regenerative medicine.

growth factor (VEGF), is beneficial for wound closure and angiogenesis. However, direct application of VEGF has not shown clear benefits in clinical trials,^[2] possibly due to the insufficient VEGF or its instability in highly proteolytic and oxidative environment of the chronic wound.^[3] The most commonly used for VEGF delivery is a heparin-based hydrogel, which has a significant drawback of a burst release in the first few hours, thus requiring the addition of large amounts of growth factors in order to maintain the long-term release.^[4] This may cause local or systemic side-effect profiles including aberrant angiogenesis, hemangioma, and tumorigenesis due to the excessive burst release.^[5] Therefore, to overcome these limitations, we sought to develop a delivery system that can continuously produce and release VEGF, which can directly stimulate angiogenesis and subsequent regeneration of the impaired diabetic wound.

A massive local inflammatory response impedes angiogenesis in diabetic wounds.^[6] The wound microenvironment is characterized by the diverse and sequential biological activity of macrophages,^[7] which polarize from a classically activated M1 phenotype with proinflammatory properties to alternatively activated M2 phenotype exhibiting anti-inflammatory and tissue repair functions. In diabetic wounds,

1. Introduction

Accelerated angiogenesis is crucial in diabetic wound healing as it provides oxygen and nutrients to the impaired tissue, alleviating uncontrolled inflammation.^[1] Delivery of exogenous angiogenic growth factors (GFs), such as vascular endothelial

Y. Lu, H. Li, M. Yao, T. Liu, G. Luo, J. Deng
Institute of Burn Research
Southwest Hospital
State Key Lab of Trauma
Burn and Combined Injury
Chongqing Key Laboratory for Disease Proteomics
Army Medical University (Third Military Medical University)
Chongqing 400038, China
E-mail: logxw@hotmail.com; djun.123@163.com

J. Wang
Department of Microbiology
Army Medical University (Third Military Medical University)
Chongqing 400038, China
E-mail: wangjing2008@aliyun.com

Y. Peng
Department of Plastic and Reconstructive Surgery
Shanghai Ninth People's Hospital
Shanghai Jiao Tong University School of Medicine
Shanghai 200011, China

Z. Li
CAS Center for Excellence in Nanoscience
Beijing Key Laboratory of Micro-Nano Energy and Sensor
Beijing Institute of Nanoenergy and Nanosystems
University of Chinese Academy of Sciences
Beijing 100083, China
E-mail: zli@binn.cas.cn

Z. Li
Department of Plastic Surgery
State Key Lab of Trauma
Burns and Combined Injury
Southwest Hospital
Army Medical University (Third Military Medical University)
Chongqing 400038, China

 The ORCID identification number(s) for the author(s) of this article can be found under <https://doi.org/10.1002/adfm.202105749>.

DOI: 10.1002/adfm.202105749

macrophages exhibit a reduced capability to induce the phenotypic switch from M1 to M2 due to hyperglycemia and presence of excessive glycosylation residues, resulting in a sustained influx and activation of proinflammatory cells.^[8] This leads to accumulation of M1 macrophages, promoting the harsh micro-environment of prolonged inflammation, strong proteolysis, and excessive oxidative stress.^[9] Therefore, a successful strategy for diabetic wound healing would simultaneously stimulate angiogenesis and modulate the macrophage polarization to reduce local inflammation.

Rapidly developing synthetic biology has enabled the application of living bacteria as biomolecule factories to treat metabolic diseases, infections, and cancer.^[10] For example, Hay et al. demonstrated an engineered bacteria expressing fibronectin (FN) and bone morphogenetic protein-2 (BMP-2) that can control stem cell growth and differentiation.^[11] Gurbatri et al. engineered a probiotic bacteria system for controlled production and intratumoral release of nanobodies targeting programmed cell death-ligand 1 (PD-L1) and cytotoxic T lymphocyte-associated protein-4 (CTLA-4), resulting in tumor regression.^[12] We proposed that nonpathogenic bacteria, specifically the lactic bacteria *Lactococcus lactis*,^[13] can be programmed with a designed gene circuit for encoding and secreting the VEGF. The lactic acid secreted by *L. lactis* could act as a metabolite signaling molecule to induce M1 macrophages toward M2-like polarization,^[14] thereby reversing the inflammatory and proteolytic characteristic of diabetic wounds.

The therapeutic effect of local administration of living bacteria is often limited by several challenges. The lack of space and environment for bacterial growth helps to reduce bacterial activity and subsequently affects production of biomolecules. Additionally, the genetically modified bacteria must be spatiotemporally restricted to reduce potential diffusion. Besides, an extracellular-mimicking environment is needed to protect and sustain release of biomolecules, especially the vulnerable growth factors. Here, a heparin-polyoxamer (HP) hydrogel with some unique advantages was synthesized for the loading of *L. lactis*. HP is a thermosensitive polymer with lower critical solution temperature, close to human body temperature,^[15] which can undergo rapid gelation with the engineered *L. lactis* and growth medium when applied on the wound, limiting the bacterial dispersal. The hydrogel is permeable to nutrients to support the bacterial growth and secretion of VEGF and lactic acid. Moreover, the hydrogel has a good affinity with VEGF due to the presence of heparin, which can stabilize, store, and sustain VEGF release. More important, in our microbial-based therapeutic device, the production and delivery of growth factors was simultaneous and dynamically persistent, which overcame the disadvantages of conventional heparin-functionalized delivery systems. The overall result of topical wound treatment with this on-site GF and macrophage polarization regulator co-delivery system strongly promoted vascularization and accelerated wound healing (Figure 1A).

2. Results and Discussion

L. lactis NZ9000, a GRAS nonpathogenic probiotic, was genetically modified by transforming a plasmid encoding VEGF

(Figure S1A,B, Supporting Information). The *veg*f gene was codon-optimized for *L. lactis* and fused to the signal peptide *usp45* secretion leader, which was driven by the inducible promoter *PnisZ*. The nisin-controlled gene expression system in *L. lactis* is based on the quorum sensor two-component system NisR and NisK, allowing the overexpression of the downstream genes after *PnisZ* (Figure 1B).^[16] As an antimicrobial peptide, nisin not only enhances the strength of the promoter but also provides a relative bacteriostatic environment to inhibit the growth of bacteria. To avoid the inhibition of engineered *L. lactis* growth, a nisin resistance gene (*nsr*) was integrated into the expression vector. We determined that 10 $\mu\text{g mL}^{-1}$ of nisin did not influence the growth of engineered *L. lactis* but inhibited the growth of wild type *L. lactis* and *Staphylococcus aureus* (a common pathogen causing skin infection) (Figure S1C, Supporting Information). As replacing proline with alanine at the N-terminus of a heterologous protein enhances its secretion,^[17] we further optimized the VEGF sequence (Figure S1D, Supporting Information), which exhibited a higher secretion (Figure S1E, Supporting Information). The secreted VEGF from medium supernatant was detected by performing a western blot (Figure 1C). The dynamic secretion of VEGF positively correlated with nisin concentration (Figure S1F, Supporting Information). Addition of inducer nisin to VEGF-secreting *L. lactis* (LL_VEGF) maximized VEGF production (≈ 6 ng per 10^9 cells) at 3 h but it gradually decreased over 24 h (Figure 1D) due to the short half-life of VEGF. Therefore, designing materials to stabilize and reduce intrinsic deactivation of the VEGF is necessary. The capacity to produce lactic acid of engineered strain was parallel with that of wild type strains (Figure 1E).

HP was successfully formed by conjugating the heparin with the mono amine-terminated polyoxamer (Figure S2A, Supporting Information), characterized by ¹H nuclear magnetic resonance (¹H NMR) (Figure S2B, Supporting Information) and Fourier transform infrared (FT-IR) spectra (Figure S2C, Supporting Information). A structural biomaterial suitable for administration on the skin wound, as a live bacterial delivery system, should have low viscosity at room (≈ 25 °C) or refrigerator temperature (≈ 4 °C), and should rapidly harden after administration. As the gelation time of polyoxamer-based hydrogels decreases along with increasing concentration, a 20% (w/v) HP copolymer solution, with the gelation time of ≈ 30 s, was chosen for probiotic delivery (Figure 1F). Thus a hybrid living hydrogel (HP@LL_VEGF) was constructed by incorporating HP and engineered VEGF-secreting *L. lactis*.

In rheology tests (Figure S2D, Supporting Information), a sol-gel phase transition process between 25 and 30 °C resulted in a sharp increase of storage modulus (G') and loss modulus (G''). Introducing LL_VEGF into the HP hydrogel did not affect the transition temperature and modulus. The storage modulus of the solidified HP@LL_VEGF (≈ 9 kPa) complies with that of skin (≈ 4.5 –8 kPa),^[18] indicating that the prepared HP thermosensitive hydrogel incorporating LL_VEGF would be a suitable skin dressing for local administration.

The spatial distribution and growing capacity of engineered probiotics in HP hydrogel were visualized using *L. lactis* expressing mCherry fluorescent protein.^[19] Scanning electron microscopy (SEM) and confocal laser scanning 3D reconstruction images showed that *L. lactis* was evenly distributed within

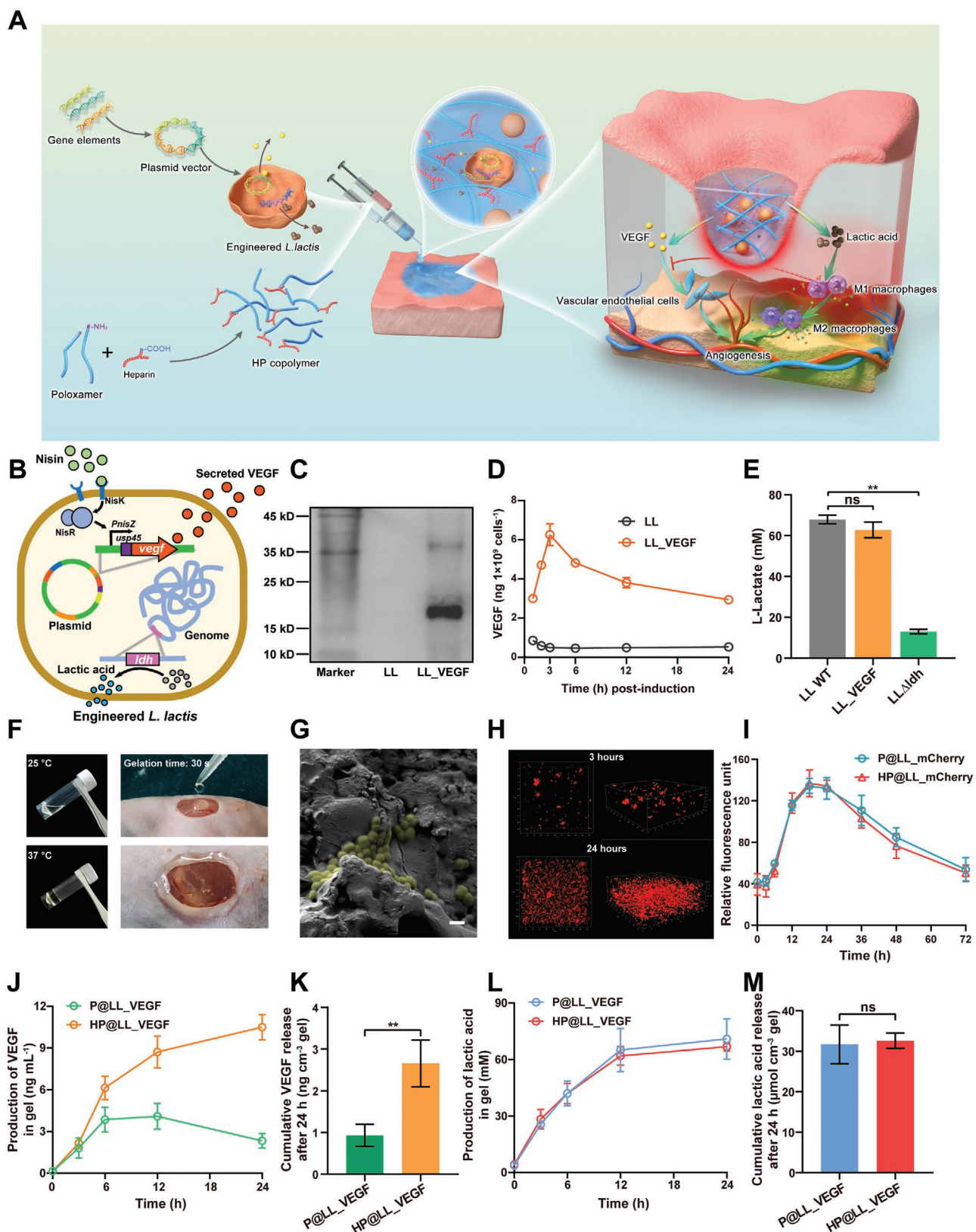


Figure 1. Engineering bacteria activated multifunctionalized hydrogel for diabetic wound repair and regeneration. A) A sketch showing the facile development of living hydrogel for accelerating angiogenesis in diabetic wounds by promoting the angiogenic capacity of endothelial cells and inducing macrophages toward M2 polarization. B) Schematic showing the design by which engineered *L. lactis* continuously secrete produced VEGF under the

the HP hydrogel (Figure 1G,H). We observed that fluorescence intensity was positively correlated with bacterial activity. Continuous measurement of fluorescence intensity inside the hydrogel demonstrated that the bacterial viability of engineered probiotics peaked at 18 h and maintained a plateau phase within 24 h. The fluorescence intensity decreased gradually after 24 h and was at half levels at 48 h when compared with the plateau value. At 72 h, the fluorescence intensity had decreased to initial levels, indicating depletion of bacterial activity (Figure 1I). These results indicated that the thermosensitive HP hydrogel supported bacterial growth and plasmid expression of engineered probiotics for at least 24 h, which maintained the bacterial activity and prolonged its retention on the skin wound. Although HP hydrogels have been used for dressings or drug delivery, their degradability has been largely overlooked. Recently, Wu et al. designed two different experimental strategies to examine HP hydrogel degradation; immersing whole hydrogels in bulk water and allowing the bottom face of the hydrogel to contact water.^[20] Within 10 days, no degradation was observed in both cases, but a slight gel dissolution had occurred at the hydrogel–water interface. The degradation rate of the poloxamer is known to be pH dependent and is thus likely coupled to lactic acid production. The degradation tests of in vitro simulation of wound administration showed gradual gel dissolution of HP and HP@LL_VEGF, with $\approx 10\%$ weight loss in 24 h. Our results were similar to Wu and the pH reduction had a slight effect on gel dissolution (Figure S3, Supporting Information).

We next sought to identify the kinetics of VEGF protein secreted from engineered probiotics inside the hydrogel using ELISA (Figure 1J). In simple poloxamer hydrogel loaded with LL_VEGF (P@LL_VEGF), the concentration of VEGF increased rapidly during the first 6 h with a peak of 4.5 ng mL^{-1} followed by a gradual decrease (Figure 1J) due to the intrinsic degradation of VEGF, which showed a similar trend as in a liquid medium (Figure 1D). Interestingly, heparin modification, which shows affinity to GFs, resulted in a continuous increase of VEGF concentration to about 10 ng mL^{-1} (Figure 1J). Further, we observed that the amount of VEGF released in the medium from the HP@LL_VEGF was significantly higher than from P@LL_VEGF after 24 h ($P < 0.01$) (Figure 1K). These results highlight the predominant biological role of heparin in protecting VEGF from deactivation, which limited VEGF diffusion and facilitated VEGF storage for local release to amplify the angiogenic signal. Moreover, lactic acid was generated sustainably from engineered probiotics for 24 h and no obvious difference was observed between the HP@LL_VEGF and P@LL_VEGF (Figure 1L,M).

Angiogenesis, the formation of new blood vessels, is a key activity during wound healing. In damaged tissue, angiogenesis

provides blood supply to support cells with nutrition and oxygen, which determines their repair and regeneration.^[21] VEGF is one of the most important proangiogenic mediators and activates various components of the angiogenic cascade.^[22] Responding to VEGF signaling, endothelial cells undergo a series of cellular activities including proliferation, migration, and differentiation to dominate the morphogenesis of blood vessels.^[23] Proliferation assay, scratch assay, and tube formation assay were conducted to verify the effect of HP@LL_VEGF on human umbilical vein endothelial cells (HUVECs) (Figure 2A).

The cell counting kit-8 (CCK8) assay revealed that viability of HUVECs was prominently enhanced after treatment of P@LL_VEGF and HP@LL_VEGF (Figure S4A, Supporting Information), and HP@LL_VEGF showed an effect stronger than P@LL_VEGF ($P < 0.05$). Compared to control and HP loaded with wild type *L. lactis* (HP@LL) groups, HP loaded with recombinant human VEGF (HP@rhVEGF, $0.1 \mu\text{g mL}^{-1}$) and HP@LL_VEGF strongly promoted endothelial cell proliferation ($P < 0.01$). There was no significant difference between the HP@rhVEGF and HP@LL_VEGF (Figure S4A, Supporting Information) ($P > 0.05$). Ki67, a marker of proliferating cells whose function is strongly associated with mitosis, was stained to confirm the trend (Figure 2B). We examined the effect of HP@LL_VEGF accelerated cell migration via scratch assay. As shown in Figure 2C and Figure S4B in the Supporting Information, addition of HP@LL_VEGF and HP@rhVEGF boosted the migration of HUVECs and expedited the closure of cell-free gaps compared to the control and HP@LL groups ($P < 0.01$), suggesting that both commercial GF and VEGF produced by engineered *L. lactis* enhanced the mobilization of HUVECs.

Using a Matrigel tube formation assay, we next evaluated the vessel-forming capability of HUVECs treated in different groups (Figure 2D). Results showed that the total tube length assessed after 24 h in HP@LL_VEGF and HP@rhVEGF groups was significantly higher than in the HP@LL and control groups ($P < 0.01$). Collectively, these results suggested that VEGF from engineered *L. lactis* promoted angiogenesis, which was comparable to the commercial GF ($P > 0.05$). Using live engineered bacteria as microbial biomolecule delivery systems is advantageous for green synthesis, incurs low cost, and shows high efficiency.^[24] Furthermore, the angiogenic effects of local application of VEGF alone with little or no effort to prepare the complex and hostile wound microenvironment was always limited.^[25]

Macrophages are the key players in the local immune responses to tissue damage and coordinate the progress and resolution of tissue repair.^[25] In impaired diabetic wounds, the proinflammatory M1 macrophages accumulate and the phenotypes switching to M2-like macrophages is dysregulated, leading to the formation of a poor regenerative environment,

induction of nisin. C) Detection of the VEGF in the supernatant via western blot. D) Level of VEGF in the supernatant at 1, 2, 3, 6, 12, and 24 h after $10 \mu\text{g mL}^{-1}$ nisin inducing ($n = 3$). E) Quantification analysis of lactic acid concentration after 12 h culture of *L. lactis* strains. F) Temperature reversible transformation and topical administration on skin wounds of HP@LL_VEGF. G) Scanning electron microscopy (SEM) of engineered probiotics encapsulated inside the HP hydrogel. Scale bar, $1 \mu\text{m}$. H) 3D laser scanning confocal micrographs of distribution and growth of LL_mCherry at 3 and 24 h. I) Quantifications of fluorescence intensity of HP@LL_mCherry along with time ($n = 3$). J) Kinetics of VEGF protein produced in P@LL_VEGF and HP@LL_VEGF using ELISA ($n = 3$). K) Cumulative VEGF released from the hydrogel after 24 h expressed as $\text{ng cm}^{-3} \text{ gel}$ ($n = 3$). L) Kinetics of lactic acid production from engineered probiotics inside the P@LL_VEGF and HP@LL_VEGF ($n = 3$). M) Cumulative lactic acid released from the hydrogel after 24 h expressed as $\mu\text{mol cm}^{-3} \text{ gel}$ ($n = 3$). ** $P < 0.01$; ns, not significant.

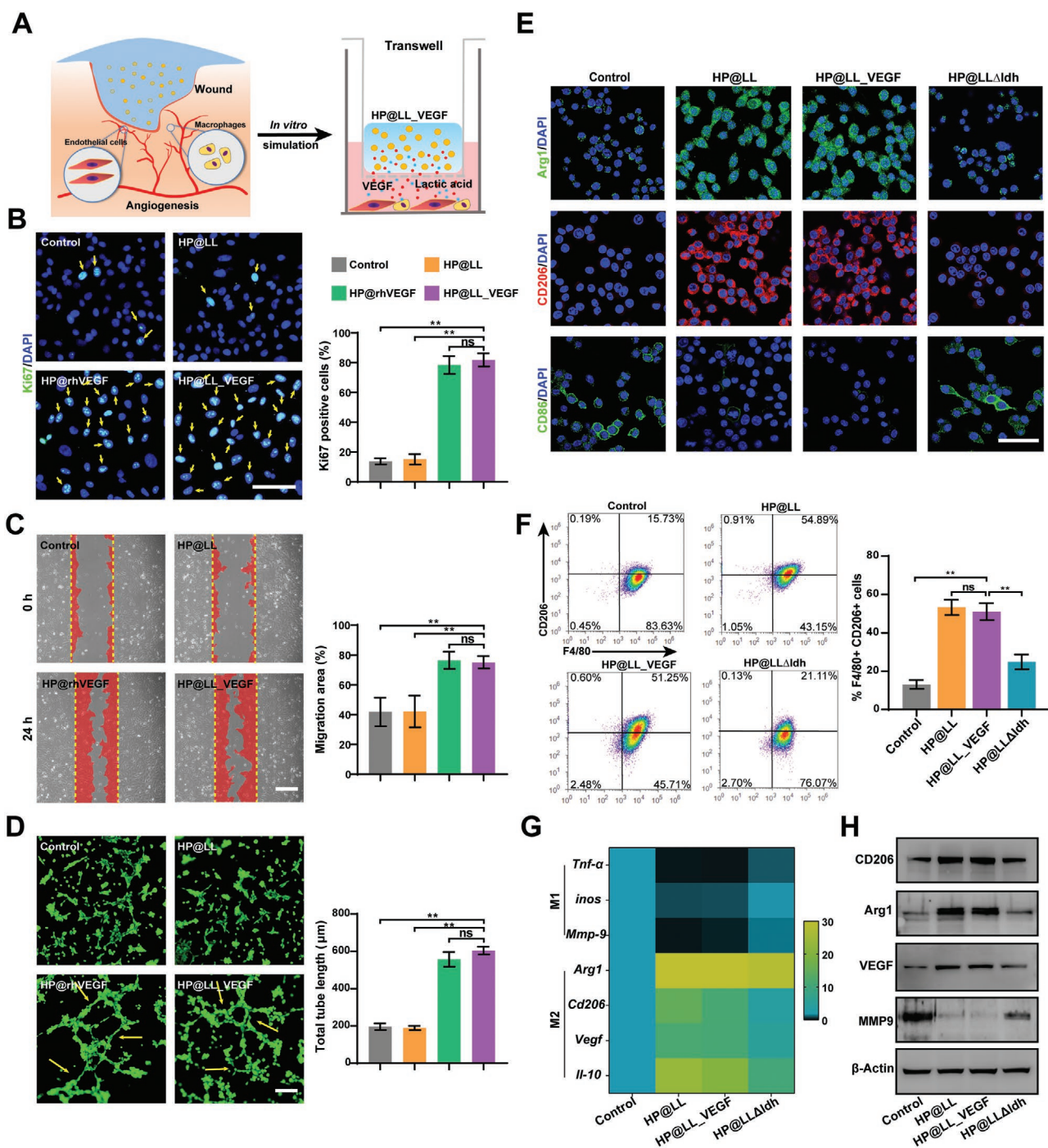


Figure 2. HP@LL_VEGF activated HUVECs and altered M1 macrophages switching to M2 phenotype in vitro. A) Illustration of the in vitro activation of vascular endothelial cells and polarization of M2 macrophages stimulated by HP@LL_VEGF. B) Representative fluorescence images of Ki67 staining (green) of HUVECs and the percentage of the Ki67-positive population ($n = 3$). Yellow arrows indicate Ki67-positive cells. Scale bar, 50 μm . C) Representative images and quantification of HUVECs migration ($n = 3$). Red area indicates the migrated cells. Scale bar, 50 μm . D) Representative images and quantitative analysis of tube formation assay in HUVECs stained with calcein-AM (green) ($n = 3$). Yellow arrows indicate the structure of vessel tubes. Scale bar, 50 μm . E) Representative fluorescence images of the macrophage phenotypes after different treatments (green: Arg1, CD86; red: CD206; blue: cell nuclear). Scale bars, 50 μm . F) Flow cytometry analysis indicating the proportion of M2 macrophages ($F4/80^+CD206^+$) ($n = 3$). G) Heat map for expression analysis (using RT-qPCR) of M1 and M2 macrophages marker genes ($n = 3$). H) Protein expression level of CD206, Arg1, VEGF, and MMP9 in macrophages determined by western blot. * $P < 0.05$ and ** $P < 0.01$; ns, not significant.

exacerbating tissue damage, and delaying wound healing.^[26] Recent evidence has demonstrated that tumor-derived lactic acid

causes a “phenotype switch,” driving M2-like gene expression in macrophages to promote tumor growth.^[27] *L. lactis* shows a

strong capability to produce lactic acid due to its high carbon flux via metabolic pathways, which are optimized to convert simple carbohydrates into lactic acid, catalyzed by lactate dehydrogenase (LDH).^[13] Quantification of lactic acid and the acidification kinetics assay confirmed that the lactic acid producing capability of engineered LL_VEGF was similar to that of a wild type, whereas it was markedly impaired in *ldh* deficient strain *L. lactis*Δ*ldh* (LLΔ*ldh*) (Figure 1E; Figure S5, Supporting Information).

We predicted that *L. lactis*, with its stronger ability to produce lactic acid, can be bioengineered to target macrophages and modulate the wound healing microenvironment. To test the hypothesis in vitro, F4/80 and CD11b (markers of macrophages) double-positive bone marrow-derived macrophages were first characterized with flow cytometry (Figure S6A, Supporting Information). Next, they were treated with lipopolysaccharide (LPS) and interferon- γ (IFN γ) to drive M1 polarization (Figures S6B,C and S7A, Supporting Information). We analyzed the changes in expression of related marker genes in macrophages after administration of HP@LL, HP@LL_VEGF, and HP loaded with LLΔ*ldh* (HP@LLΔ*ldh*). Mannose receptor (MMR, CD206) and ARG1, associated with M2-like macrophage phenotype, as well as CD86, a marker of M1 macrophages, were stained by immunofluorescence (Figure 2E). Confocal laser scanning microscope images showed that HP@LL and HP@LL_VEGF significantly induced the expression of CD206 and ARG1 on the cell membrane and in the cytoplasm, respectively, whereas control and HP@LLΔ*ldh* groups displayed weak fluorescence intensity. Furthermore, the expression of CD86 was downregulated in response to HP@LL and HP@LL_VEGF administration. The effect of lactic acid producing *L. lactis* on induction of M2-like phenotype was similar to that observed by adding 30×10^{-3} M pure L-lactic acid (Figures S7B, S8, and S9, Supporting Information).

Flow cytometry was performed to quantitatively analyze the proportion of M2-like macrophages (F4/80⁺, CD206⁺) during M1 polarization and our results verified the trend observed thus far (Figure 2F). Moreover, real-time quantitative PCR (RT-qPCR) and western blot were performed to detect the mRNA and protein level expressions of M1 markers (related to pro-inflammation and proteolysis; TNF- α , iNOS, and MMP9), M2 markers (anti-inflammatory; ARG1 and CD206), and other anti-inflammatory and angiogenic markers (IL-10, VEGF). The relative mRNA expression of M1 markers was significantly decreased, whereas that of M2 markers was promoted in the HP@LL and HP@LL_VEGF groups than in the other groups (Figure 2G; Figure S10, Supporting Information) ($P < 0.01$). Furthermore, the protein expression results from the western blot were consistent with the results of RT-qPCR (Figure 2H). In addition, the function of VEGF and HP hydrogel in altering macrophages polarization had been excluded (Figure S11, Supporting Information).

Lactic acid from *L. lactis* induced M2 polarization of macrophages in a dose-dependent manner as observed by adding different concentrations of *L. lactis* culture medium supernatant (Figure S12, Supporting Information). These results indicated that *L. lactis*, with its strong capacity to produce lactic acid, would promote macrophages switching to M2 phenotype and the deficiency of *ldh* would attenuate this effect. Specifically,

reduction of M1 macrophage-derived inflammatory mediators (such as TNF- α), nitric oxide, iNOS, and proteases (such as MMP9) modulates the wound environment to relieve the tissue damage and improve growth signaling. Increase in M2 macrophage-related ARG1, which produces ornithine to facilitate cell proliferation and VEGF production, further supplemented the angiogenic effect of engineered probiotics, thereby improving the tissue regeneration and recovery potential.

Our initial in vivo experiments aimed to demonstrate the viability and distribution of HP@LL_VEGF on the cutaneous wound following topical administration. We used LL_mCherry to track plasmid expression and bacterial retention. Following in situ application of LL_mCherry alone and in combination with HP hydrogel (HP@LL_mCherry) in living mice, fluorescence expressions were visualized and quantified using an in vivo imaging system (IVIS). As shown in Figure 3A, the rapid decrease of fluorescence intensity in LL_mCherry alone indicated that probiotics were eliminated quickly and thus, adhered poorly to the wound site, suggesting significant shortening of the effective time. It is challenging to restrict bacteria into the target site, and protect them from the complex immune environment without a bacterial-supportive medium.^[28] In combination with the hydrogel, the probiotics were restricted locally in the wound, plasmid expression peaked at 12 h, and lasted for at least 24 h (Figure 3B). These results implied that HP hydrogel overcame the spatiotemporal challenge of bacterial growth and activity. We also evaluated the capacity of HP@LL_VEGF in on-site retaining nisin and producing VEGF in wounds (Figure S13, Supporting Information). A large proportion of the cationic nisin could be retained within the negatively charged HP hydrogel, allowing for the enhancement of VEGF production. Next, the distribution and amounts of engineered probiotics were visualized in the cryosections collected at different time points (Figure 3C). We observed that engineered probiotics were mainly distributed in the hydrogel. We combined the limited nutrition and physical encapsulation of hydrogel materials to reduce bacterial spread and increase biocontainment in 24 h.

To investigate whether probiotics loaded in HP hydrogel could elicit acute inflammatory response, we first monitored the local inflammation-induced hyperemia using noninvasive laser speckle contrast analysis (LASCA) for blood flow (Figure S14A, Supporting Information). Cutaneous wound induction increased inflammation. Interestingly, the hyperemia around the wound decreased after the topical application of HP@LL and HP@LL_VEGF ($P < 0.05$) (Figure S14B, Supporting Information), indicating that immune response was ameliorated. Moreover, the expression of genes related to inflammation, including *Il-1 β* , *Nf- κ b*, *Nos2*, and *Tnf- α* did not increase significantly. In contrast, HP@LL and HP@LL_VEGF partially reduced the activation of *Nf- κ b* and *Tnf- α* compared to the control wound ($P < 0.05$) (Figure S14C, Supporting Information). These results confirmed that probiotics in hydrogel applied to open wounds could partially reduce the local inflammation. Risks of systemic infection and inflammation were excluded analyzing the white blood cells, lymphocytes (LYM), and monocytes (MONO) in peripheral blood (Figure S14D, Supporting Information). Systemic acid–base balance was maintained, as the serum lactate level was not notably different between the groups (Figure S14E, Supporting Information).

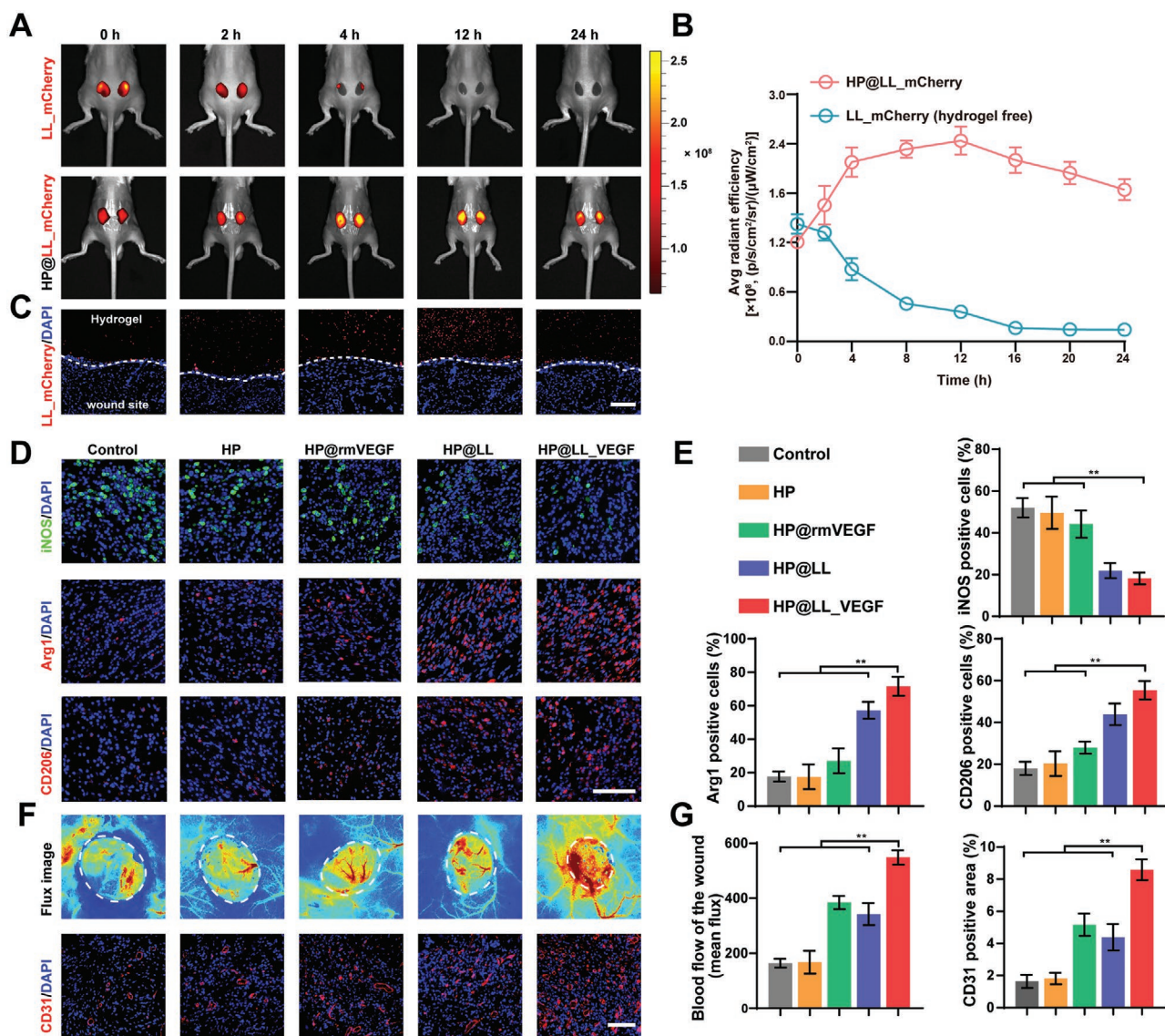


Figure 3. Effects of HP@LL_VEGF on bacterial growth, macrophage polarization, and angiogenesis in vivo. A) Representative images and B) quantification of retention and plasmid expression of LL_mCherry alone and with HP@LL_VEGF after in situ application on the wounds using an in vivo imaging system (IVIS) ($n = 3$). C) Representative images of in vivo distribution of engineered probiotics on the wound tissue. Scale bar, 50 μm . D) Representative images of iNOS (M1 macrophages) and Arg1 and CD206 (M2 macrophages) immunofluorescence staining on day 6 (green: iNOS; red: Arg1 and CD206; blue: cell nuclear). Scale bar, 100 μm . E) Statistical data of the percentage of iNOS⁺, Arg1⁺, and CD206⁺ macrophages ($n = 3$). F) Representative images of blood flow in the wounds on day 6 and CD31 immunofluorescence on day 12. Scale bar, 100 μm . G) Statistical data of blood flow of the wounds ($n = 3$) and CD31 positive area in the wound tissue ($n = 3$). ** $P < 0.01$.

The open wounds, especially in diabetic patients, are prone to bacterial infection, resulting in production of proinflammatory mediators by the recruited immune cells (neutrophils and macrophages).^[29] Thus, biological safety is vital when live bacteria are applied in the therapeutics and biomedicine, which determines their clinical and translational applicability. In our study, *L. lactis* administration did not show any symptoms of infection due to its probiotic nature, while the biocompatible hydrogel relatively isolated the microorganism, thereby preventing it from entering the wound tissue and ensuring the biosafety, which highlights its potential application in clinical management of wounds, especially in diabetic patients.

We hypothesized that enhanced proliferation, migration, and vessel-forming capability of endothelial cell as well as M2 polarization of macrophages stimulated by HP@LL_VEGF in vitro would translate to angiogenesis and accelerate wound healing in vivo. To test the efficacy of HP@LL_VEGF in healing chronic wounds, a diabetic mouse with full-thickness skin defect was chosen. Diabetic mouse wounds were treated by HP hydrogel, HP@LL, HP@rmVEGF, and HP@LL_VEGF once a day. The untreated mice were taken as controls.

A key challenge in treating chronic wounds is the persistence of the chronic inflammatory stage, while normal wounds exhibit acute inflammation that resolves in a few days.^[30]

Inability of macrophages to switch from a proinflammatory to an anti-inflammatory phenotype combined with persistent inflammation is a hallmark of diabetic wounds.^[31] Therefore, we performed immunofluorescence staining of macrophages in wound sections during the proliferation phase (day 6) to elucidate the *in vivo* effect of HP@LL_VEGF in inducing M1 macrophages to M2 phenotype. As shown in Figure 3D,E, administration of HP@LL and HP@LL_VEGF significantly decreased the proportion of iNOS M1 marker positive cells, whereas the infiltration and distribution of CD206 and Arg1 M2 markers positive cells was enhanced compared to the other groups that did not produce lactic acid ($P < 0.01$). In wound healing, M2 macrophages promote the recovery of regeneration potential via secreting anti-inflammatory mediators and releasing angiogenic and GF. Our results further confirmed that HP@LL_VEGF could drive the shift in macrophage phenotype for tissue repair and regeneration.

Insufficient angiogenesis is a key cause of impaired healing of diabetic wounds.^[32] To investigate the effect of HP@LL_VEGF in promoting angiogenesis, blood flow at the diabetic wound sites was monitored using LASCA. Compared to the other treatments, the wounds treated with HP@LL_VEGF

displayed a significantly higher blood perfusion ($P < 0.01$). Immunofluorescence staining of CD31, the marker of the vascular endothelial cells involved in neovascularization, was performed for histological analysis of angiogenesis. An increased CD31 positive area, representing the vascular structure, was observed in the HP@LL_VEGF group ($P < 0.01$) (Figure 3F,G). HP@rmVEGF and HP@LL treatments too showed positive effects on increasing the CD31 positive area, but their effects were inferior to that of HP@LL_VEGF treatment. These results demonstrated that treatment with HP@LL_VEGF re-established structural and functional blood vessels network in wounds.

A diabetic mouse model was first established by feeding mice a high-fat and high-sugar diet and by streptozotocin (STZ) injection (Figure S15A, Supporting Information). We observed that diabetic mouse wounds were difficult to heal even after 20 days, whereas wounds in normal mice healed in 12 days (Figure S15B, Supporting Information). Digital photographs of wounds showed that mice treated with HP@LL_VEGF exhibited significantly faster wound closure compared to the other groups, with nearly 50% closure achieved on day 6 (Figure 4A–C). On day 12, ≈90% wound closure was achieved

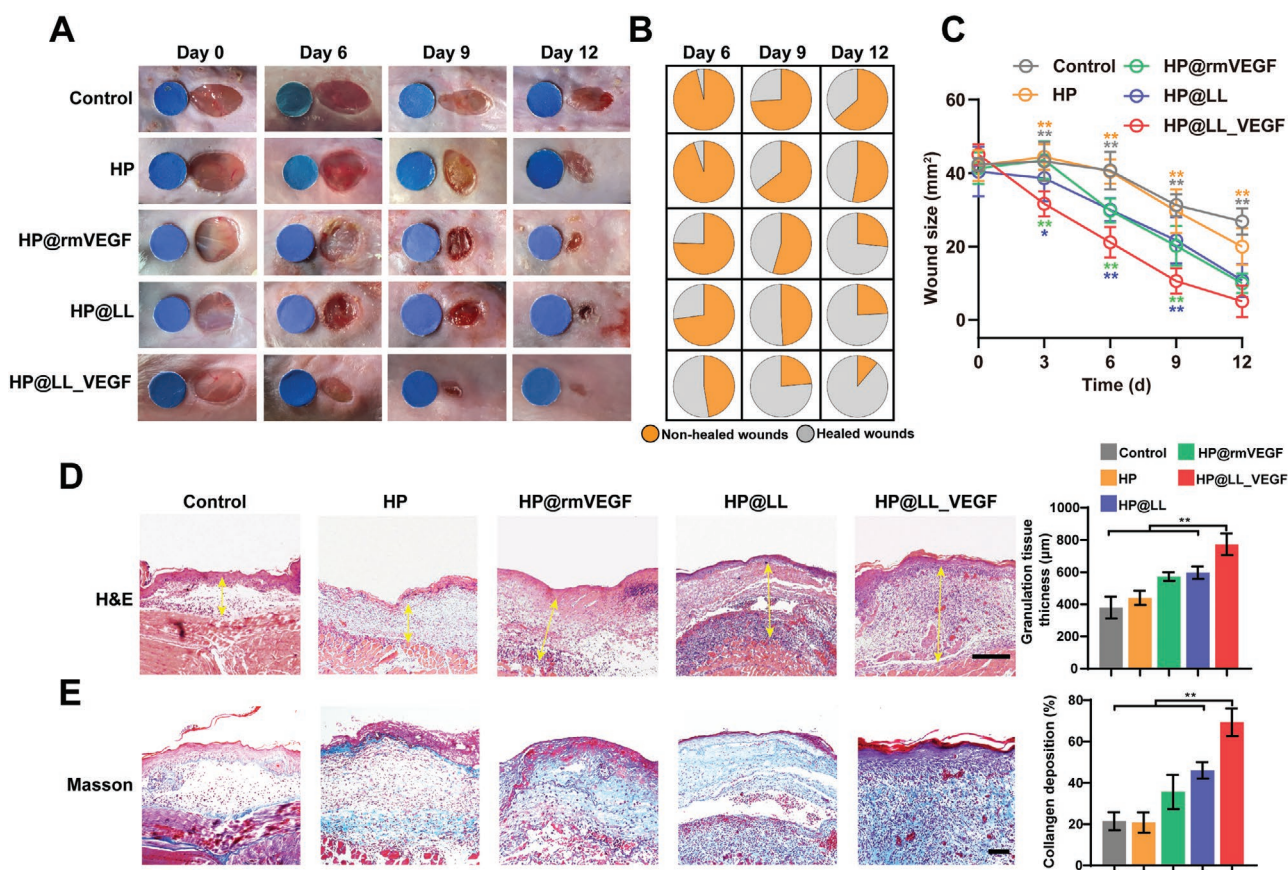


Figure 4. HP@LL_VEGF promoted diabetic wound repair and regeneration *in vivo*. A) Representative digital images of the wound area in response to different treatments on day 0, day 6, day 9, and day 12. The round blue card with a 6 mm diameter indicates initial wound size. B) Fractions of the wounds healed by the different treatments on day 6, day 9, and day 12 ($n = 6$). C) Quantitative analysis of wound area for each group ($n = 6$). Asterisks with colors represent comparisons of corresponding groups versus HP@LL_VEGF group. D) H&E staining of the wound area reflected the granulation tissue on day 12 ($n = 3$). Yellow arrows indicate thickness of granulation tissue. Scale bar, 100 μm . E) Masson staining of the wound area reflected collagen deposition on day 12 ($n = 3$). Scale bar, 100 μm . * $P < 0.05$ and ** $P < 0.01$.

with HP@LL_VEGF treatment, whereas only $\approx 30\text{--}50\%$ closure was achieved in the control and HP groups, and $\approx 70\text{--}80\%$ closure was achieved in the HP@LL and HP@rmVEGF groups. Moreover, addition of the experimental concentrations of nisin did not significantly affect the wound healing of the mouse model (Figure S15C, Supporting Information). Thus, the accelerated wound healing would mainly benefit from the delivery of VEGF and the phenotypic regulation of macrophages. And lactic acid from *L. lactis* had no significant effect on blood sugar level (Figure S15D, Supporting Information).

Granulation tissue formation and tissue maturation were evaluated histologically 12 days after inflicting wounds by measuring granulation tissue thickness and collagen deposition. Histology analysis revealed that HP@LL_VEGF treatment significantly increased the granulation tissue thickness compared to other groups ($P < 0.01$) (Figure 4D). Massive collagen deposition, indicating recovery and maturation from damaged tissues, was observed in HP@LL_VEGF-treated wounds ($P < 0.01$) (Figure 4E).

These data showed that therapeutic effect of HP@LL_VEGF outperformed other groups. Further, this confirmed that the combination of the direct enhancement of growth signals and indirect modulation of immune responses is an efficient and promising strategy to treat delayed cutaneous wound healing observed in diabetic conditions.

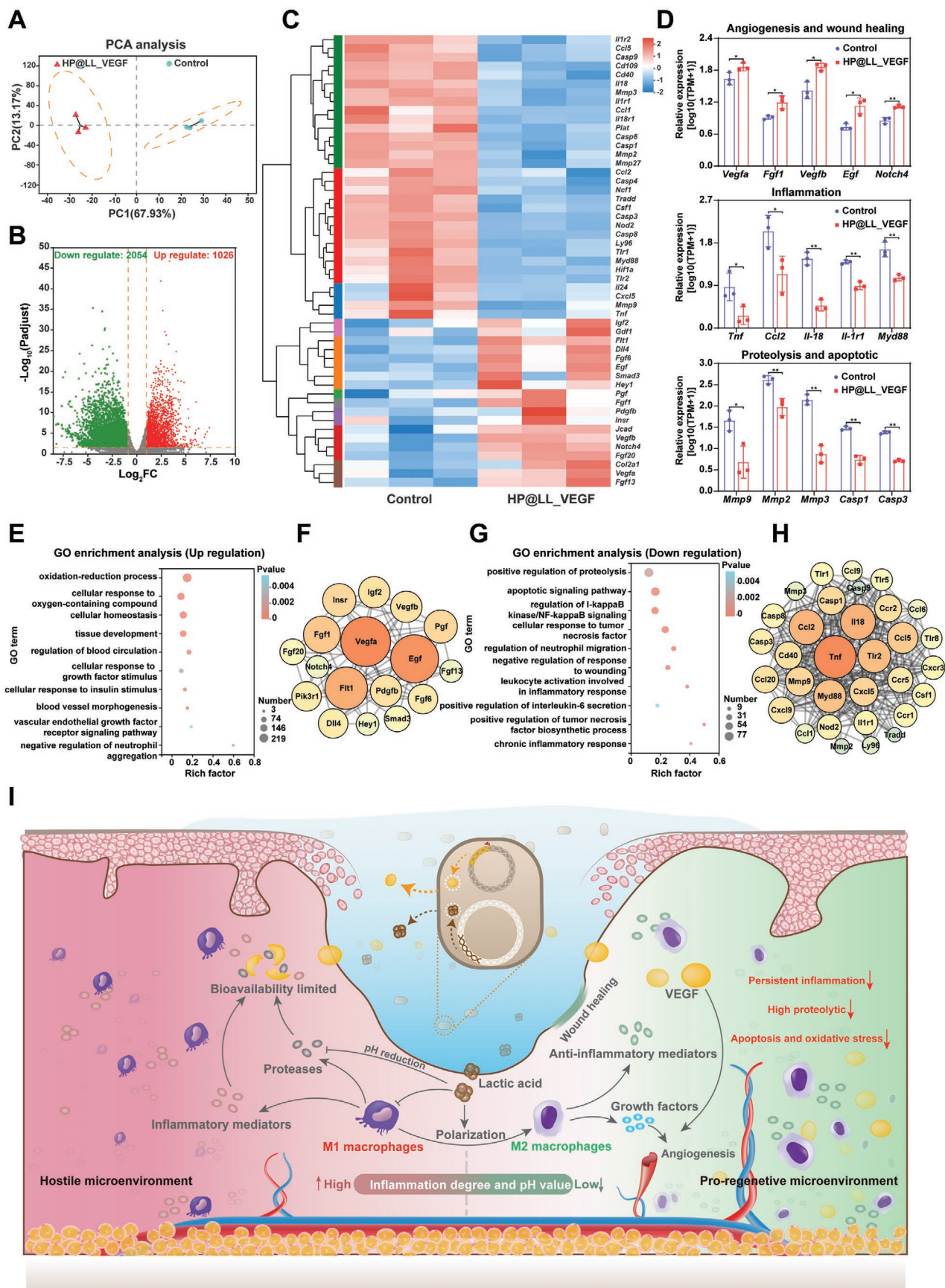
For global assessment of diabetic wound microenvironment after treatment with HP@LL_VEGF, RNA-sequencing (RNA-seq) was performed on samples collected from wound tissue on day 6, which indicates transition from the inflammatory phase to proliferation phase during normal wound healing. Tissue from untreated diabetic wounds was taken as control. A significant difference between the transcriptomic profiles of the control and HP@LL_VEGF-treated groups was observed by the unguided principal component analysis (PCA) (Figure 5A). After administration of HP@LL_VEGF, 3080 significant differentially expressed genes (DEGs) were identified, with 1026 upregulated and 2054 downregulated genes, according to the empirical Bayes method (fold change ≥ 4 ; q value < 0.05), as showed in the volcano plots (Figure 5B).

Enrichments analysis based on DEGs were conducted for up- and downregulation gene sets. Hierarchical cluster analysis separated and screened the gene expression differences between the wound tissue from control and HP@LL_VEGF-treated mice (Figure 5C). Specifically, the expressions of genes related to angiogenesis and wound healing (*Vegfa*, *Fgf1*, *Vegfb*, *Egf*, and *Notch4*) were upregulated after the HP@LL_VEGF treatment, whereas the expressions of genes related to inflammation (*Tnf*, *Ccl2*, *Il-18*, *Il-1r1*, and *Myd88*), proteolysis (*Mmp9*, *Mmp2*, and *Mmp3*), and apoptosis (*Casp1* and *Casp3*) were significantly downregulated (Figure 5D; Figure S16, Supporting Information). Gene ontology (GO) analysis revealed that the 1026 upregulated genes focused on cellular homeostasis, cellular response to oxygen and GF, and blood vessel and tissue morphogenesis (Figure 5E). Kyoto Encyclopedia of Genes and Genomes (KEGG) pathway enrichment analysis revealed that HP@LL_VEGF-treatment enhanced the signal transduction of cGMP-PKG, VEGF, and PPAR pathways, which enhanced angiogenesis (Figure S17A,C, Supporting Information). These results suggested that the regenerative potential was restored in

treated diabetic wounds and showed positive response to growth signals. The protein–protein interactions network analysis not only identified the central role of VEGF but also demonstrated the important role played by the adjacent EGF, FLT1, and FGF1 in interacting with leading proteins to exert the therapeutic effects and accelerate wound healing in response to HP@LL_VEGF treatment (Figure 5F). Furthermore, the 2054 down-regulated genes were closely related to the pathological process associated with diabetic wounds. GO and KEGG analysis showed that the key enrichment items focused on ameliorating inflammation (e.g., reduction of neutrophil migration and leukocyte activation, negative regulation of chemokines, and pro-inflammatory factors signaling pathways), protecting cells from apoptosis and damage (e.g., downregulation of MAPK, TNF, and apoptotic signaling pathways), and weakening the proteolysis and hyperglycemia reaction (e.g., inhibition of MMPs and AGE-RAGE signaling pathway) (Figure 5G; Figure S17B,D, Supporting Information). Notably, TNF, which activates the cascade of inflammation and necrosis,^[33] dominated the protein interaction networks hindering the process of wound healing, suggesting that HP@LL_VEGF attenuates the hostile wound microenvironment by inhibiting the TNF signaling pathway (Figure 5H; Figure S17, Supporting Information).

As shown in Figure 5I, our study aimed to elucidate the etiology and microenvironment of diabetic wounds and develop a promising avenue for promoting angiogenesis in diabetic wounds. This was achieved by utilizing engineered probiotics encapsulated in hydrogel to locally produce and deliver proangiogenic factor (VEGF) and macrophage-regulated mediator (lactic acid). In the bacteria-supporting and GF protecting HP hydrogel, engineered *L. lactis* equipped with an artificially designed gene circuit continuously secretes VEGF, thereby providing continuous angiogenic growth signal. *L. lactis* alters the phenotype shift of macrophages by producing lactic acid. The polarization of accumulated M1 macrophages to M2 breaks the hostile status of proinflammatory, proteolytic, and apoptotic wound microenvironment. Further, pH reduction resulting from lactic acid production potentiated the retention of VEGF due to inhibition of the enzymatic activity of plasmin, which mainly cleaves and inactivates VEGF (Figure S18, Supporting Information).^[34] HP@LL_VEGF mainly promotes the secretion of EGF, FGF, PGF, and other growth factors and upregulates key regeneration-related genes such as Smad3 and Notch4 by activating VEGF signal, cGMP-PKG, PPAR, and other pathways to accelerate angiogenesis and wound healing. At the same time, HP@LL_VEGF inhibit TNF, MAPK, chemokines, apoptosis, and other signaling pathways, downregulate the expression of Ccl2, IL-18, Casp3, MMP family, and other genes, and reverse the adverse regenerative environment of diabetic wounds. Collectively, these effects improved the bioavailability of VEGF and reinforced the angiogenic signals. Therefore, our strategy drove the functional reconstruction of vessel networks and promoted the rapid regeneration of diabetic wounds.

Here, we demonstrated that VEGF and lactic acid, expressed and delivered by engineered probiotics for diabetic wound healing, enabled local therapeutic angiogenesis in diabetic mouse models. Moreover, we showed that VEGF and lactic acid can be adapted into other biological circuits due to their protected storage and release using an HP@LL_VEGF delivery



system, which serves to confine the bacterial population and inhibit bacterial entry into the impaired tissue site, thereby minimizing the risk of systemic toxicities.

Some biodegradable matrices, glycosaminoglycans (GAGs), and extracellular matrix (ECM)-derived proteins, such as fibronectin and fibrin, have been developed as controlled release systems for VEGF delivery. The most commonly used system is a heparin-based hydrogel.^[35] However, these systems follow a fixed preloading/release pattern and temporal imbalance, which has the significant drawback of producing a burst release in the first few hours, thus requiring the addition of large amounts of growth factors in order to maintain the long-term release.^[4] Supraphysiological levels of these molecules due to the excessive burst release, coupled with poor delivery kinetics, are probably responsible for the various side effects, low effectiveness, and extra costs of these approaches.^[5] Regarding the translational potential of our HP@LL_VEGF delivery system, all the materials we selected were FDA-approved or biocompatible. Our therapeutic system resulted in sustained delivery, prolonged retention of therapeutic biomolecules, and spatial restriction of bacteria once administrated on the wounds. These features will be helpful in a clinical setting, where minimally invasive and self-sustained therapies are desirable.

Although several combination approaches have been explored for angiogenesis, immunotherapies are often more effective when combined with other proangiogenesis reagents.^[36] Microbial-based therapeutic platforms are highly modular and convenient for the rapid engineering of multiple payloads that can be delivered as a combination of probiotic strains. Angiogenesis is essential for the reconstruction of skin function in diabetic wound treatment. Many biomaterials have been designed to promote diabetic wound recovery by enhancing vascularization. Chen et al. reported an oxygen-producing patch, which improved neovascularization by up to 1.7 times in a splinted excisional dermal wound model of diabetic mice.^[37] Wang et al. prepared an injectable multifunctional hydrogel containing MnO₂ nanosheets that could increase vascular density up to 1.6 times in diabetic mice wounds.^[38] Ouyang et al. reported a black phosphorus-based gel with near-infrared light responsiveness, to promote the proliferation of endothelial cells, vascularization, and angiogenesis by up to 2.8 times in wounds in diabetic mice. Xiao et al. reported copper-based nanoparticles with a slow Cu²⁺ release rate, which enhanced vascularization by up to 2.0 times in diabetic mice wounds.^[39] Soto et al. reported a NO-releasing implant, which increased blood vessel densities by 0.5 and 0.7 times in healthy and diabetic pigs, respectively.^[40] Lucas et al. reported a modified anti-miR-92a that could be activated by light to increase angiogenesis by up to 2.8 times in diabetic mice wounds.^[41] In

this work, we developed a living microbial-based therapeutic device to raise blood vessel density by up to 5.5 times in the diabetic wounds of diabetic mice, a rate which is markedly higher than those previously reported. Therefore, future iterations of this platform, combined with delivery system such as our HP@LL_VEGF, can be programmed to produce a wide variety of immunotherapeutic and other agents to test a variety of rational therapeutic combinations. Furthermore, we are exploring chromosome integrated expressing system to replace plasmids, which would remove extra genetic elements and perform more efficiently. Last, to improve the system's clinical relevance, other routes of therapeutic administration in more translational animal models need to be considered.

3. Conclusion

Currently, the clinical nonsurgical treatment of diabetic wounds mainly involves blood glucose control, wound debridement, and wound dressing. The most commonly used wound dressings are hydrocolloids, hydrogels, and foam dressings, which can absorb wound exudates, but which lack bioactive molecules to modulate the wound microenvironment.^[42] Despite the fact that some bioactive molecules, such as growth factors, stem cells, and platelet-rich plasma, have been used clinically to treat diabetic wounds, they face problems, such as easy deactivation, low bioavailability, and unitary wound microenvironment regulation.^[43] Thus, the development of novel wound dressings, which could effectively and steadily release bioactive molecules to regulate the wound microenvironment is urgently needed. The HP@LL_VEGF hydrogel, which can simultaneously and steadily release bioactive proteins and immune-regulating molecules, meets the above-mentioned clinical needs, and paves the way engineering probiotic-based bioactive molecule delivery systems to promote diabetic wound healing. We have built a stable biological circuit integrated into a probiotic with therapeutic analogues as a potential standard treatment for optimization toward clinical translation. The HP@LL_VEGF system should help advance the angiogenesis therapy field by reducing inflammatory microenvironments and stimulating angiogenesis simultaneously. Moreover, sustained production of therapeutic components combined with minimized toxicity would facilitate improved immunotherapeutic and GF co-delivery to a broader range of chronic wounds.

4. Experimental Section

For detailed experimental conditions, methods of synthesis, and the additional characterizations, please see Figures S1–S18 in the

Figure 5. Global assessments of the diabetic wound microenvironment after treatment with HP@LL_VEGF using RNA-seq. A) Principal component analysis (PCA) was performed based on differentially expressed genes (DEGs) in the wound tissue of the two groups. B) Volcano plots showing the upregulated and downregulated genes in response to HP@LL_VEGF treatment. C) Heat map of upregulated and downregulated genes in the diabetic wound microenvironment after HP@LL_VEGF treatment (fold change ≥ 4 and $P < 0.05$). D) Relative expression of genes related to the processes crucial for diabetic wound regeneration, including angiogenesis, inflammation, proteolysis, and apoptosis ($n = 3$). E) Gene ontology (GO) enrichment analysis of the upregulated genes. F) Protein–protein interaction network of upregulated genes involved in angiogenesis and wound healing. G) GO enrichment analysis of all the downregulated genes. H) Protein–protein interaction network of downregulated genes involved in pathophysiological features of diabetic wound. I) Illustration of postulated mechanism by which HP@LL_VEGF modulated the wound microenvironment for accelerated angiogenesis and wound regeneration.

Supporting information. All animal experiments were performed according to protocols approved by the Laboratory Animal Welfare and Ethics Committee of Army Medical University (Third Military Medical University), No. AMUWEC20201397.

Supporting Information

Supporting Information is available from the Wiley Online Library or from the author.

Acknowledgements

This work was supported by the National Natural Science Foundation of China (81920108022, 61875015, T2125003 and 81630055), the Natural Science Foundation of Chongqing (cstc2020jcyj-msxmX1057), the State Key Laboratory of Trauma, Burn and Combined Injury, Army Medical University (Grant Nos. SKLYQ202001 and SKLKF201703), the Beijing Natural Science Foundation (JQ20038), and the Fundamental Research Funds for the Central Universities. The authors would like to thank Yan Chen and Doudou Chen from Shiyanjia Lab (www.shiyanjia.com) for their help in drawing the TOC.

Conflict of Interest

The authors declare no conflict of interest.

Data Availability Statement

Research data are not shared.

Keywords

angiogenesis, drug delivery, living hydrogels, synthetic biology, wound healing

Received: July 9, 2021

Published online:

- [1] a) D. G. Armstrong, A. J. M. Boulton, S. A. Bus, *N. Engl. J. Med.* **2017**, *376*, 2367; b) V. Falanga, *Lancet* **2005**, *366*, 1736; c) D. Marino, J. Luginbühl, S. Scola, M. Meuli, E. Reichmann, *Sci. Transl. Med.* **2014**, *6*, 221ra14.
- [2] a) Y. Crawford, N. Ferrara, *Cell Tissue Res.* **2009**, *335*, 261; b) Z. G. Zhang, L. Zhang, Q. Jiang, R. Zhang, K. Davies, C. Powers, N. Bruggen, M. Chopp, *J. Clin. Invest.* **2000**, *106*, 829.
- [3] a) D. Duscher, E. Neofytou, V. W. Wong, Z. N. Maan, R. C. Rennert, M. Inayathullah, M. Januszyk, M. Rodrigues, A. V. Malkovskiy, A. J. Whitmore, G. G. Walmsley, M. G. Galvez, A. J. Whittam, M. Brownlee, J. Rajadas, G. C. Gurtner, *Proc. Natl. Acad. Sci. USA* **2015**, *112*, 94; b) S. W. Tas, C. X. Maracle, E. Balogh, Z. Szekanecz, *Nat. Rev. Rheumatol.* **2016**, *12*, 111.
- [4] a) U. Freudenberg, A. Zieris, K. Chwalek, M. V. Tsurkan, M. F. Maitz, P. Atallah, K. R. Levental, S. A. Eming, C. Werner, *J. Controlled Release* **2015**, *220*, 79; b) L. Abune, Y. Wang, *Trends Pharmacol. Sci.* **2021**, *42*, 300.
- [5] a) X. Huang, C. S. Brazel, *J. Controlled Release* **2001**, *73*, 121; b) C. R. Ozawa, A. Banfi, N. L. Glazer, G. Thurston, M. L. Springer, P. E. Kraft, D. M. McDonald, H. M. Blau, *J. Clin. Invest.* **2004**, *113*, 516; c) A. J. Whittam, Z. N. Maan, D. Duscher, V. W. Wong, J. A. Barrera, M. Januszyk, G. C. Gurtner, *Adv Wound Care* **2016**, *5*, 79.
- [6] S. A. Eming, P. Martin, M. Tomic-Canic, *Sci. Transl. Med.* **2014**, *6*, 265sr6.
- [7] T. A. Wynn, K. M. Vannella, *Immunity* **2016**, *44*, 450.
- [8] P. Krzyszczyk, R. Schloss, A. Palmer, F. Berthiaume, *Front. Physiol.* **2018**, *9*, 419.
- [9] a) D. L. Laskin, V. R. Sunil, C. R. Gardner, J. D. Laskin, *Annu. Rev. Pharmacol. Toxicol.* **2011**, *51*, 267; b) H. Wu, F. Li, W. Shao, J. Gao, D. Ling, *ACS Cent. Sci.* **2019**, *5*, 477.
- [10] M. R. Charbonneau, V. M. Isabella, N. Li, C. B. Kurtz, *Nat. Commun.* **2020**, *11*, 1738.
- [11] J. J. Hay, A. Rodrigo-Navarro, M. Petaroudi, A. V. Bryksin, A. J. García, T. H. Barker, M. J. Dalby, M. Salmeron-Sanchez, *Adv. Mater.* **2018**, *30*, 1804310.
- [12] C. R. Gurbatri, I. Lia, R. Vincent, C. Coker, S. Castro, P. M. Treuting, T. E. Hinchliffe, N. Arpaia, T. Danino, *Sci. Transl. Med.* **2020**, *12*, eaax0876.
- [13] N. Mao, A. Cubillos-Ruiz, D. E. Cameron, J. J. Collins, *Sci. Transl. Med.* **2018**, *10*, eaao2586.
- [14] a) D. Zhang, Z. Tang, H. Huang, G. Zhou, C. Cui, Y. Weng, W. Liu, S. Kim, S. Lee, M. Perez-Neut, J. Ding, D. Czyz, R. Hu, Z. Ye, M. He, Y. G. Zheng, H. A. Shuman, L. Dai, B. Ren, R. G. Roeder, L. Becker, Y. Zhao, *Nature* **2019**, *574*, 575; b) J. Zhang, J. Muri, G. Fitzgerald, T. Gorski, R. Gianni-Barrera, E. Masschelein, G. D'Hulst, P. Gilardoni, G. Turiel, Z. Fan, T. Wang, M. Planque, P. Carmeliet, L. Pellerin, C. Wolfrum, S. M. Fendt, A. Banfi, C. Stockmann, I. Soro-Arnáiz, M. Kopf, K. De Bock, *Cell Metab.* **2020**, *31*, 1136.
- [15] R. Li, Y. Li, Y. Wu, Y. Zhao, H. Chen, Y. Yuan, K. Xu, H. Zhang, Y. Lu, J. Wang, X. Li, X. Jia, J. Xiao, *Biomaterials* **2018**, *168*, 24.
- [16] I. Mierau, M. Kleerebezem, *Appl. Microbiol. Biotechnol.* **2005**, *68*, 705.
- [17] L. Steidler, S. Neiryck, N. Huyghebaert, V. Snoeck, A. Vermeire, B. Goddeeris, E. Cox, J. P. Remon, E. Remaut, *Nat. Biotechnol.* **2003**, *21*, 785.
- [18] N. Lohmann, L. Schirmer, P. Atallah, E. Wandel, R. A. Ferrer, C. Werner, J. C. Simon, S. Franz, U. Freudenberg, *Sci. Transl. Med.* **2017**, *9*, eaai9044.
- [19] J. Huang, S. Liu, C. Zhang, X. Wang, J. Pu, F. Ba, S. Xue, H. Ye, T. Zhao, K. Li, Y. Wang, J. Zhang, L. Wang, C. Fan, T. K. Lu, C. Zhong, *Nat. Chem. Biol.* **2019**, *15*, 34.
- [20] J. Wu, J. Zhu, C. He, Z. Xiao, J. Ye, Y. Li, A. Chen, H. Zhang, X. Li, L. Lin, Y. Zhao, J. Zheng, J. Xiao, *ACS Appl. Mater. Interfaces* **2016**, *8*, 18710.
- [21] M. L. Kang, H. S. Kim, J. You, Y. S. Choi, B. J. Kwon, C. H. Park, W. Baek, M. S. Kim, Y. J. Lee, G. I. Im, J. K. Yoon, J. B. Lee, H. J. Sung, *Sci. Adv.* **2020**, *6*, eaay5413.
- [22] J. Ishihara, A. Ishihara, K. Fukunaga, K. Sasaki, M. J. V. White, P. S. Briquez, J. A. Hubbell, *Nat. Commun.* **2018**, *9*, 2163.
- [23] S. P. Herbert, D. Y. Stainier, *Nat. Rev. Mol. Cell Biol.* **2011**, *12*, 551.
- [24] a) P. Praveschotinunt, A. M. Duraj-Thatte, I. Gelfat, F. Bahl, D. B. Chou, N. S. Joshi, *Nat. Commun.* **2019**, *10*, 5580; b) X. Wang, J. Pu, B. An, Y. Li, Y. Shang, Z. Ning, Y. Liu, F. Ba, J. Zhang, C. Zhong, *Adv. Mater.* **2018**, *30*, 1705968.
- [25] S. J. Forbes, N. Rosenthal, *Nat. Med.* **2014**, *20*, 857.
- [26] K. Hamidzadeh, S. M. Christensen, E. Dalby, P. Chandrasekaran, D. M. Mosser, *Annu. Rev. Physiol.* **2017**, *79*, 567.
- [27] a) Q. W. Chen, J. W. Wang, X. N. Wang, J. X. Fan, X. H. Liu, B. Li, Z. Y. Han, S. X. Cheng, X. Z. Zhang, *Angew. Chem., Int. Ed. Engl.* **2020**, *59*, 21562; b) O. R. Colegio, N. Q. Chu, A. L. Szabo, T. Chu, A. M. Rhebergen, V. Jairam, N. Cyrus, C. E. Brokowski, S. C. Eisenbarth, G. M. Phillips, G. W. Cline, A. J. Phillips, R. Medzhitov, *Nature* **2014**, *513*, 559.

- [28] a) A. C. Anselmo, K. J. McHugh, J. Webster, R. Langer, A. Jaklenec, *Adv. Mater.* **2016**, *28*, 9486; b) T. C. Tang, E. Tham, X. Liu, K. Yehl, A. J. Rovner, H. Yuk, C. de la Fuente-Nunez, F. J. Isaacs, X. Zhao, T. K. Lu, *Nat. Chem. Biol.* **2021**, *17*, 724.
- [29] L. P. da Silva, R. L. Reis, V. M. Corrello, A. P. Marques, *Annu. Rev. Biomed. Eng.* **2019**, *21*, 145.
- [30] S. A. Eming, T. A. Wynn, P. Martin, *Science* **2017**, *356*, 1026.
- [31] A. E. Boniakowski, A. S. Kimball, B. N. Jacobs, S. L. Kunkel, K. A. Gallagher, *J. Immunol.* **2017**, *199*, 17.
- [32] S. Kargozar, F. Baino, S. Hamzehlou, M. R. Hamblin, M. Mozafari, *Chem. Soc. Rev.* **2020**, *49*, 5008.
- [33] G. Opendakker, J. Van Damme, J. J. Vranckx, *Trends Immunol.* **2018**, *39*, 341.
- [34] P. Vempati, A. S. Popel, F. M. Gabhann, *Cytokine Growth Factor Rev.* **2014**, *25*, 1.
- [35] a) M. Mochizuki, E. Güç, A. J. Park, Z. Julier, P. S. Briquez, G. A. Kuhn, R. Müller, M. A. Swartz, J. A. Hubbell, M. M. Martino, *Nat. Biomed. Eng.* **2020**, *4*, 463; b) V. Sacchi, R. Mittermayr, J. Hartinger, M. M. Martino, K. M. Lorentz, S. Wolbank, A. Hofmann, R. A. Largo, J. S. Marschall, E. Groppa, R. Gianni-Barrera, M. Ehrbar, J. A. Hubbell, H. Redl, A. Banfi, *Proc. Natl. Acad. Sci. USA* **2014**, *111*, 6952; c) Y. Niu, Q. Li, Y. Ding, L. Dong, C. Wang, *Adv. Drug Delivery Rev.* **2019**, *146*, 190.
- [36] L. R. Nih, S. Gojgini, S. T. Carmichael, T. Segura, *Nat. Mater.* **2018**, *17*, 642.
- [37] H. Chen, Y. Cheng, J. Tian, P. Yang, X. Zhang, Y. Chen, Y. Hu, J. Wu, *Sci. Adv.* **2020**, *6*, eaba4311.
- [38] S. Wang, H. Zheng, L. Zhou, F. Cheng, Z. Liu, H. Zhang, L. Wang, Q. Zhang, *Nano Lett.* **2020**, *20*, 5149.
- [39] a) J. Ouyang, X. Ji, X. Zhang, C. Feng, Z. Tang, N. Kong, A. Xie, J. Wang, X. Sui, L. Deng, Y. Liu, J. S. Kim, Y. Cao, W. Tao, *Proc. Natl. Acad. Sci. USA* **2020**, *117*, 28667; b) J. Xiao, Y. Zhu, S. Huddleston, P. Li, B. Xiao, O. K. Farha, G. A. Ameer, *ACS Nano* **2018**, *12*, 1023.
- [40] R. J. Soto, E. P. Merricks, D. A. Bellinger, T. C. Nichols, M. H. Schoenfisch, *Biomaterials* **2018**, *157*, 76.
- [41] T. Lucas, F. Schäfer, P. Müller, S. A. Eming, A. Heckel, S. Dimmeler, *Nat. Commun.* **2017**, *8*, 15162.
- [42] a) S. Matoori, A. Veves, D. J. Mooney, *Sci. Transl. Med.* **2021**, *13*, eabe4839; b) H. Cho, M. R. Blatchley, E. J. Duh, S. Gerecht, *Adv. Drug Delivery Rev.* **2019**, *146*, 267.
- [43] a) Q. Bai, K. Han, K. Dong, C. Zheng, Y. Zhang, Q. Long, T. Lu, *Int. J. Nanomed.* **2020**, *15*, 9717; b) H. X. Hua, H. B. Deng, X. L. Huang, C. Q. Ma, P. Xu, Y. H. Cai, H. T. Wang, *Oxid. Med. Cell. Longevity* **2021**, *2021*, 8831535.